

Supporting Information

Ultra-small pH-responsive Nd-doped NaDyF₄ Nanoagents for Enhanced Cancer Theranostic by *in situ* Aggregation

Yuxin Liu^{†a}, Huimin Fan^{†a}, Quanwei Guo^a, Anqi Jiang^a, Xiaoxia Du^b, Jing Zhou^{*a}

[a] Department of Chemistry, Capital Normal University, Beijing, 100048, P. R. China.

[b] Shanghai Key Laboratory of Magnetic Resonance, Physics Department, East China Normal University, Shanghai 200062, P. R. China.

E-mail: Jingzhou@cnu.edu.cn (J. Zhou)

† These authors contribute equal to this work.

EXPERIMENTAL SECTION

Characterization: The sizes and morphologies of NaDyF₄:x%Nd (x = 2.5, 5, 10, 20) and NaDyF₄:10%Nd-GA-Fe were determined using a Tecnai G²F30 transmission electron microscope (TEM) under 300 kV accelerating. Samples were dispersed in cyclohexane and water dropped on the surface of a copper grid. Energy-dispersive X-ray analysis (EDXA) and selected area electron diffraction (SAED) of the NaDyF₄:x%Nd (x = 2.5, 5, 10, 20) were also performed during TEM measurements. Ultraviolet-visible-near infrared (UV-vis-NIR) absorption spectra were obtained on a Shimadzu UV-3600 UV-vis-NIR spectrophotometer. All samples were homogenized by vortex before UV-vis-NIR spectra determination. Powder X-ray diffraction (XRD) measurement was measured with a Bruker D8 advance X-ray diffractometer from 10° to 70° (Cu K α radiation, $\lambda = 1.54 \text{ \AA}$). Zeta potential and hydrodynamic diameter was measured on a Zetasizer nano 90. To ensure the accuracy of size distribution measurement, great care was taken to eliminate dust from the sample. The aqueous solution of the GA-coated NaDyF₄:x%Nd (x = 2.5, 5, 10, 20) and NaDyF₄:10%Nd-GA-Fe was filtered through two membrane filters with 0.45 μm nominal pore size connected in series. Near-infrared second window downconversion luminescence (NIR II DCL) spectra were measured with a Maya LIFS-808 fluorescence spectrometer by using an external 0-7 W 808 nm adjustable laser as the excitation source. Fourier transform infrared (FTIR) spectra were measured using a Fourier Transform Infrared Spectrophotometer IRPRESTIGE-21 (Shimadzu) from samples in KBr pellets.

Cell culture: CCC-HEL-1 (human normal liver cells) and HCT-116 (human colon carcinoma cells) cell lines were provided by the Institute of Basic Medical Sciences Chinese Academy of Medical Sciences. Cells were grown in DMEM (Dulbecco's modified Eagle's medium) supplemented with 10% FBS (fetal bovine serum) and 1% penicillin-streptomycin at 37°C with 5% CO₂. Cultures were maintained at 37°C under a humidified atmosphere containing 5% CO₂. For use in the experiments, 1×10^5 cells well⁻¹ were seeded in 10 mm glass

coverslips and allowed to attach for 24 h prior to the assay. For cell staining assays, CCC-HEL-1 and HCT116 cells were incubated with the NaDyF₄:10%Nd-GA-Fe (300 ppm) for 1 h at 37°C in a serum-free medium.

r₁ and r₂ relaxivities measurement: The T₁-weighted MR signal intensity of NaDyF₄:x%Nd (x = 2.5, 5, 10, 20) in tubes were ascertained by the average intensity in the defined regions of interests. r₁ relaxivities were performed in a 0.5 T (Shanghai Niumag Corporation ration NM120-Analyst). The values of r₁ were calculated through the curve fitting of 1/T₁ relaxation time (s⁻¹) vs the Dy³⁺ concentration (mM) or particle mass concentration (mg mL⁻¹). The slope of the line provides the r₁. The T₂-weighted MR signal intensity of NaDyF₄:x%Nd (x = 2.5, 5, 10, 20), NaDyF₄:10%Nd-GA-Fe, and NaDyF₄:10%Nd-CA-Fe in tubes were ascertained by the average intensity in the defined regions of interests. r₂ relaxivities were performed in a 0.5 T (Shanghai Niumag Corporation ration NM120-Analyst). The values of r₂ were calculated through the curve fitting of 1/T₂ relaxation time (s⁻¹) vs the Dy³⁺ concentration (mM) or particle mass concentration (mg mL⁻¹). The slope of the line provides the r₂.

In vitro T₂-weighted MRI: The T₂-weighted MR images were obtained using a 3 T Siemens Magnetom Trio running on Siemens' Syngo software version B15 (Siemens Medical Systems), in conjunction with an 8 array Loop coil (Siemens Medical Systems). Different concentration of NaDyF₄:x%Nd (x = 2.5, 5, 10, 20), NaDyF₄:10%Nd-GA-Fe solution, NaDyF₄:10%Nd-GA-Fe-incubated cells, and NaDyF₄:10%Nd-CA-Fe-incubated cells were placed in a 1.5 mL tubes. The following parameters were adopted: a spin-echo sequence: a repetition time (TR) of 3000 ms, echo time (TE) of 20.3 ms, Flip angle = 120°, slice thickness = 2.0 mm, FOV read = 200 mm, and base resolution = 256.

In vivo T₂-weighted MRI: All animal procedures were in agreement with institutional animal use and care committee and carried out ethically and humanely. HCT116 tumor-bearing nude mice were used for the *in vivo* imaging experiment. Before imaging, the mouse was anesthetized and set on homemade mount. T₂-weighted MRI *in vivo* was conducted using a

spin-echo sequence under 3 T (TR = 3000 ms, TE = 20.3 ms, slice thickness = 2.0 mm, FOV read = 200 mm, base resolution = 256). The mice were scanned before and after the administration of contrast agent. The mice were injected with the solution of NaDyF₄:10%Nd-GA-Fe intravenously (10 mg per kg body weight of mouse) or intratumorally (2 mg per kg body weight of mouse). T₂-weighted MR coronal cross-section images were obtained within 120 min post-injection. NaDyF₄:10%Nd-CA-Fe was used for comparison.

In vivo photothermal imaging: Photothermal imaging was performed before and after the intravenous NaDyF₄:10%Nd-GA-Fe injection (10 mg per kg body weight of mouse). Photothermal images were acquired and analyzed by FLIR software.

Tissue distribution: After intravenously injected with NaDyF₄:10%Nd-GA-Fe (n = 5, dose = 10 mg per kg body weight of mouse), tissues were harvested from nude mice bearing HCT116 tumors 1 hour and 4 hours post-injection. By breaking up the tissues (heart, spleen, lungs, kidneys, liver, and tumor) respectively, the centrifuging resultant liquid was dissolved in DI water (1 mL), and diluted with DI water to 1:10 v/v. Determination of Dy³⁺ uptake content in tissues was performed by inductively coupled mass spectroscopy (ICP-MS) analysis (Agilent 7500ce ICP-MS).

In vivo photothermal therapy (PTT): When the tumor size reached ~1.0 cm³, nude mice bearing HCT116 tumors were randomly divided in to four groups for PTT. The nanoagents was injected intravenously from caudal vein (dose = 10 mg per kg body weight of mouse). The power intensity of laser during PTT was fixed at 0.64 W cm⁻². The tumor sizes were measured by a caliper every two or three days after photothermal treatment and calculated according to the formulation: The tumor volume = (tumor length) × (tumor width)²/2.

MTT assays: HCT116 and CCC-HEL-1 cells (90 μL well⁻¹, 10⁵ mL⁻¹) were seeded into 96-well cell culture plate, respectively, and the cells were incubated at 37°C under 5% CO₂ for 24 hours. Medium of NaDyF₄:10%Nd-GA-Fe (10 μL well⁻¹, containing 1% PBS) at

concentrations of 0-300 mg mL⁻¹ were added to the wells of the experimental group, and medium containing 1% PBS (10 µL well⁻¹) to the control group. The cells were incubated at 37 °C under 5% CO₂ within 24 and 48 hours, respectively. Subsequently, 3-(4,5-Dimethylthiazol-2-yl)-2,5-diphenyltetrazolium bromide (MTT, 10 µL, 5 mg mL⁻¹) was added to each well of the 96-well assay plate and incubated for an additional 4 hours. After the addition of dimethyl sulfoxide (DMSO, 100 µL well⁻¹), the assay plate was allowed to stand at room temperature for 30 min. Tecan Infinite M200 monochromator-based multifunction microplate reader was used to measure the OD570 (*Abs* value) of each well with background subtraction. The following formula was used to calculate the viability of cells growth.

Cell viability (%) = (mean of *Abs.* value of treatment group/mean *Abs.* value of control) ×100%.

Hematology studies: Blood was harvested from mice intravenously injected with NaDyF₄:10%Nd-GA-Fe (n = 5, dose = 20 mg per kg body weight of mouse) and from mice receiving no injection (n = 5, dose = 0 mg per kg body weight of mouse, control), 24 hours, 7 days, 30 days, and 60 days post-injection, respectively. Blood was collected from the orbital sinus by quickly removing the eye ball from the socket with a pair of tissue forceps. Five important hepatic indicators (ALT, alanine aminotransferase; AST, aspartate amino transferase; TBIL, total bilirubin; ALB, albumin; TP, Total protein), and two indicators for kidney functions (UA, uric acid; CREA, Creatinine) were measured. Blood smears were prepared by placing a drop of blood on one end of a slide, and using another slide to disperse the blood along the length of the slide. The slide was left to air dry, after which the blood was stained with hematoxylin and eosin (H&E).

H&E stained tissues: The heart, liver, spleen, lung, and kidney were harvested from mice intravenously injected with NaDyF₄:10%Nd-GA-Fe (n = 5, dose= 20 mg per kg body weight of mouse) and from mice receiving no injection (n = 5, dose = 0 mg per kg body weight of

mouse, control), 24 hours, 7 days, 30 days, and 60 days post-injection, respectively. The tissues were fixed in paraformaldehyde, embedded in paraffin, sectioned, and stained with H&E. The histological sections were observed under an optical microscope.

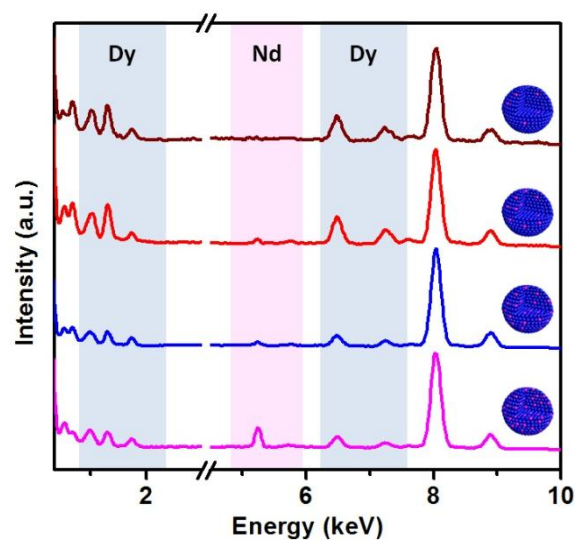


Figure S1. EDXA spectra of hydrophobic NaDyF₄:x%Nd (x = 2.5, 5, 10, 20) nanoagents.

Table S1. The Dy and Nd amount in nanoagents measured by ICP-MS. Cal. represent the Dy/Nd ratio calculated from ICP-MS results. The. represent the theoretical Dy/Nd ratio.

| nanoagents | Dy amount (%) | Nd amount (%) | Dy/Nd (cal.) | Dy/Nd (the.) |
|----------------------------|---------------|---------------|--------------|--------------|
| NaDyF ₄ :2.5%Nd | 97.374 | 2.626 | 37.08 | 39 |
| NaDyF ₄ :5%Nd | 95.102 | 4.898 | 19.42 | 19 |
| NaDyF ₄ :10%Nd | 89.251 | 10.749 | 8.30 | 9 |
| NaDyF ₄ :20%Nd | 79.655 | 20.345 | 3.92 | 4 |

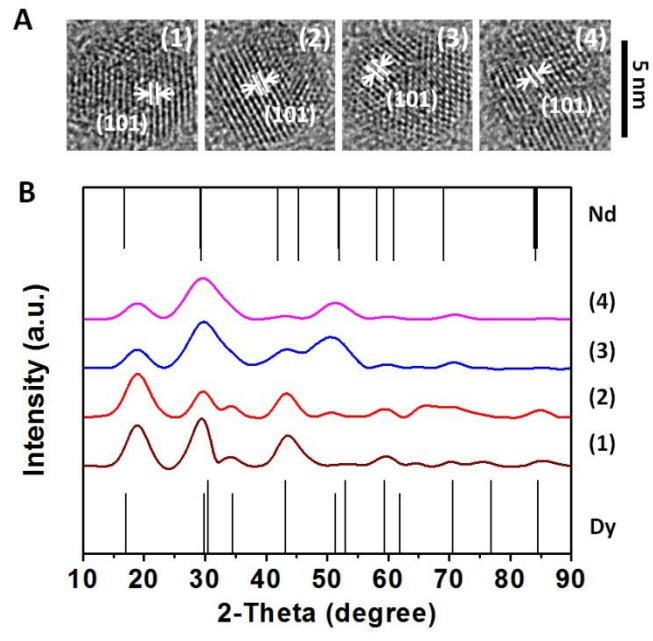


Figure S2. HR-TEM images A) and XRD patterns B) of $\text{NaDyF}_4:x\%\text{Nd}$ $x = 2.5$ (1), 5 (2), 10 (3), and 20 (4). (Dy: $\beta\text{-NaDyF}_4$, JCPDS: 27-0687; Nd: $\beta\text{-NaNdF}_4$, JCPDS: 35-1367).

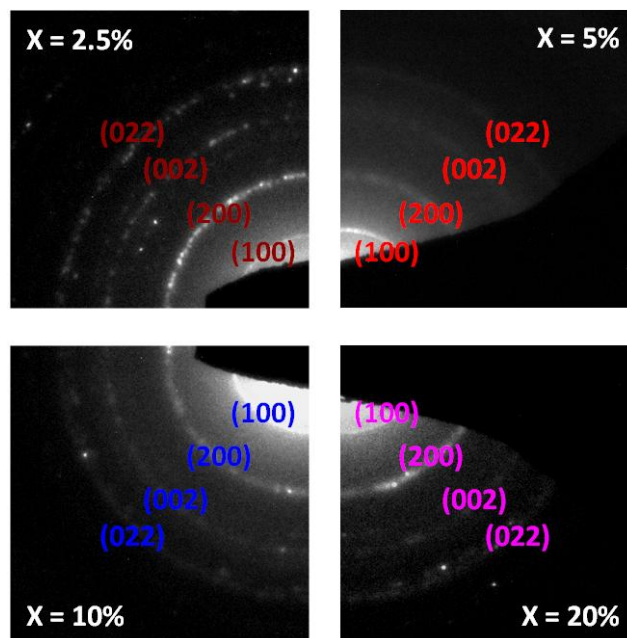


Figure S3. SAED patterns of hydrophobic NaDyF₄:x%Nd (x = 2.5, 5, 10, 20) nanoagents.

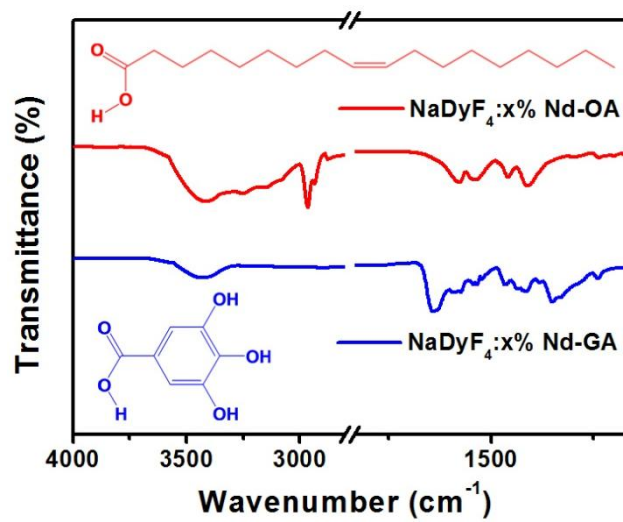


Figure S4. Fourier transform infrared (FTIR) spectra of $\text{NaDyF}_4:10\% \text{Nd-OA}$ and $\text{NaDyF}_4:10\% \text{Nd-GA}$.

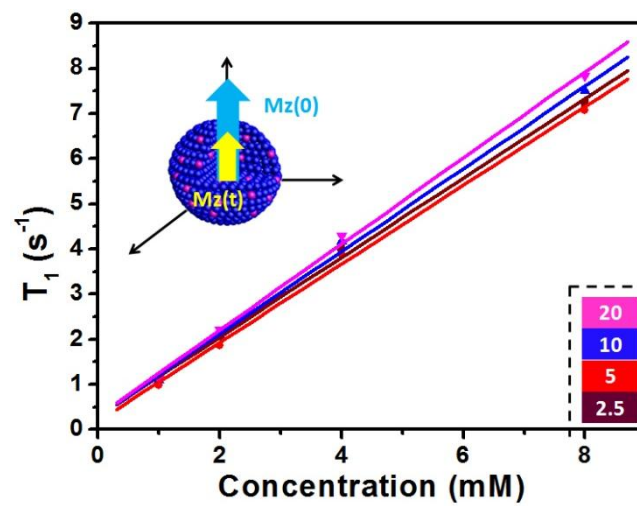


Figure S5. Longitudinal relaxivity (r_1) of NaDyF₄:x%Nd (x = 2.5, 5, 10, 20) nanoagents.

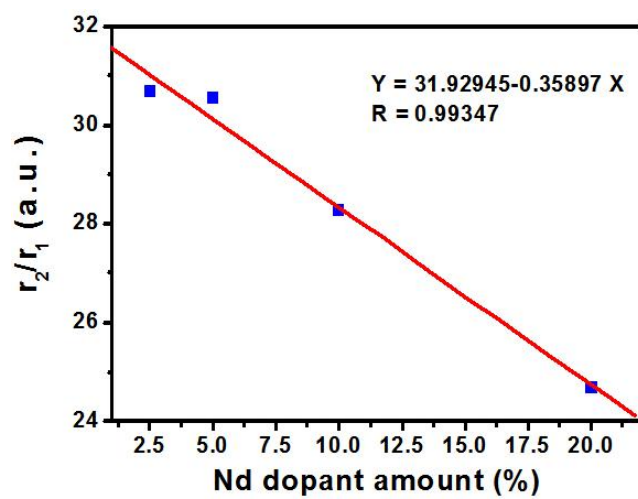


Figure S6. r_2/r_1 vs Nd dopant amount of $\text{NaDyF}_4:x\% \text{Nd}$ ($x = 2.5, 5, 10, 20$) nanoagents.

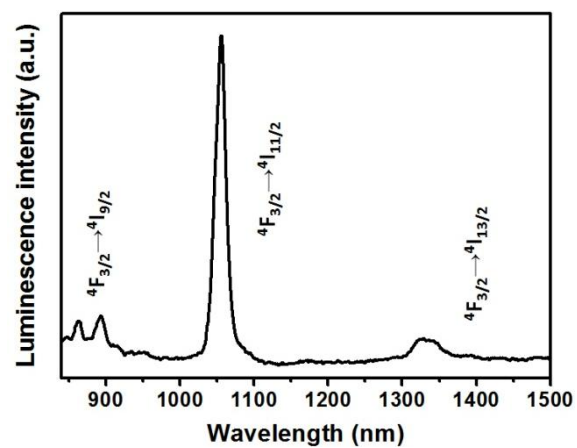


Figure S7. The luminescence spectrum of NaDyF₄:10%Nd-GA-Fe in the NIR range of 840 nm to 1500 nm.

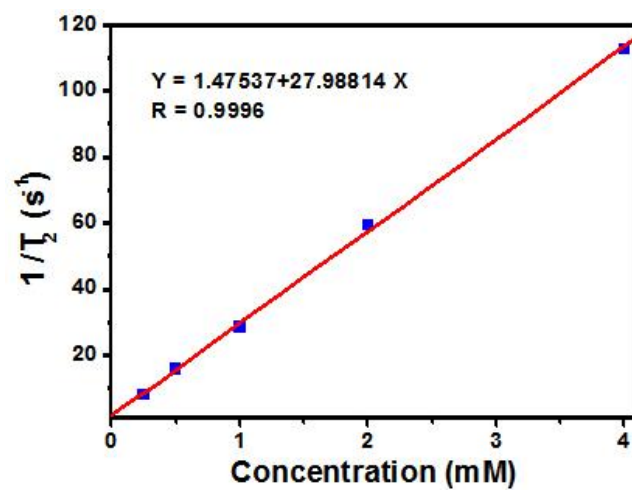


Figure S8. Relaxation rate ($1/T_2$) vs various mass concentrations of $\text{NaDyF}_4:10\%\text{Nd-GA-Fe}$ at room temperature using a 0.5 T MRI scanner.

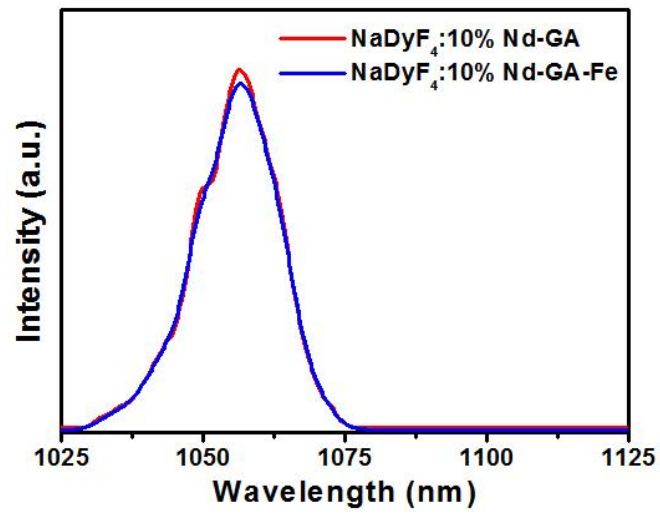


Figure S9. NIR II DCL spectra of NaDyF₄:10%Nd-GA-Fe and NaDyF₄:10%Nd-GA.

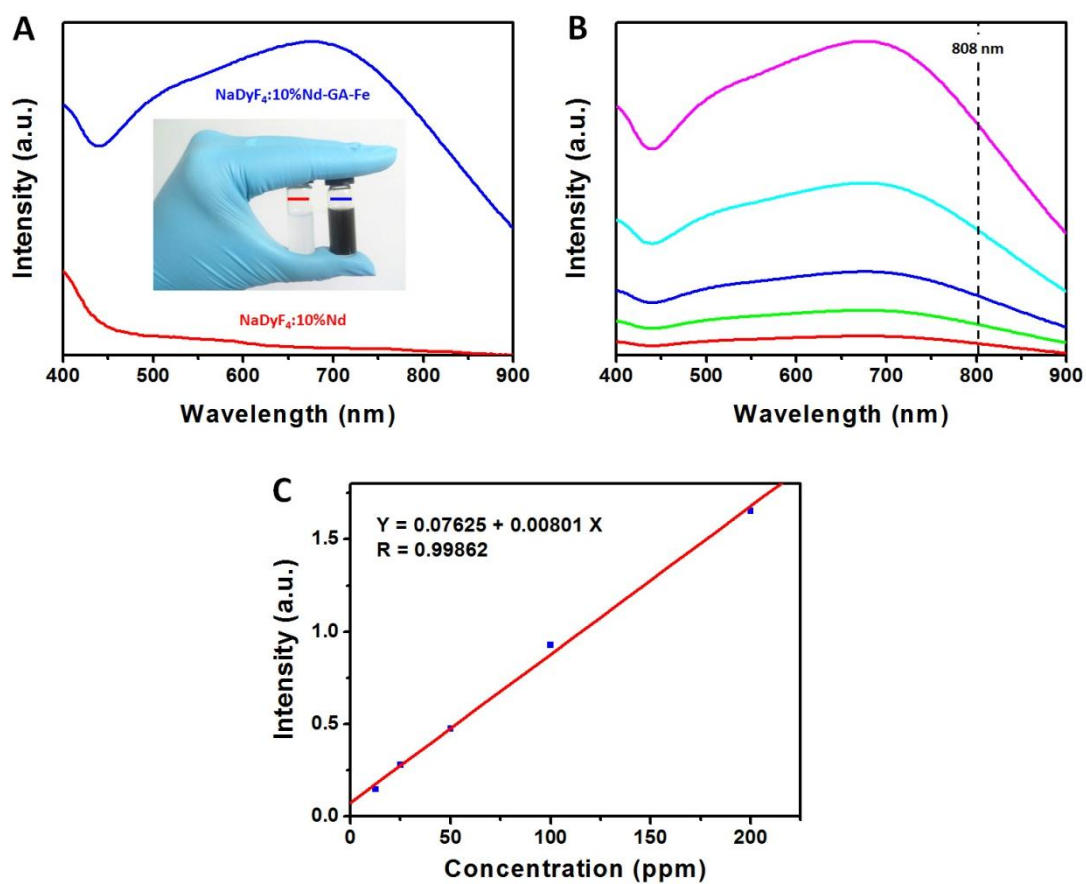


Figure S10. UV-vis-NIR absorption of NaDyF₄:10%Nd and NaDyF₄:10%Nd-GA-Fe (200 ppm, A), and NaDyF₄:10%Nd-GA-Fe at different concentration (12.5-200 ppm, B). C) A linear relationship for the optical absorbance at 808 nm as a function of the concentration of NaDyF₄:10%Nd-GA-Fe.

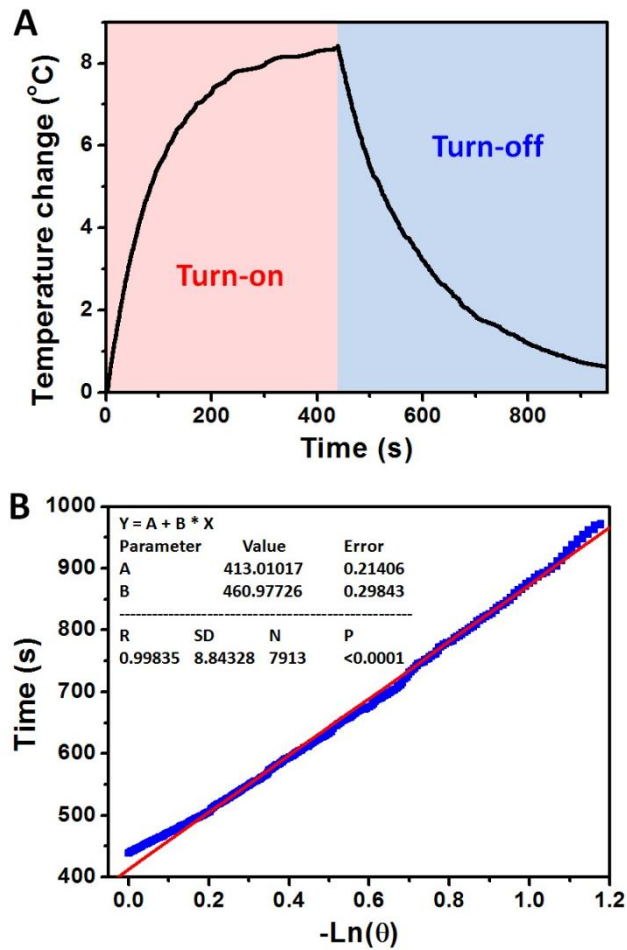


Figure S11. A) Turn-on and turn-off heating curves of 200 ppm NaDyF₄:10%Nd-GA-Fe solution. B) Linear time data vs $-\ln\theta$ obtained from the cooling period upon 808 nm irradiation.

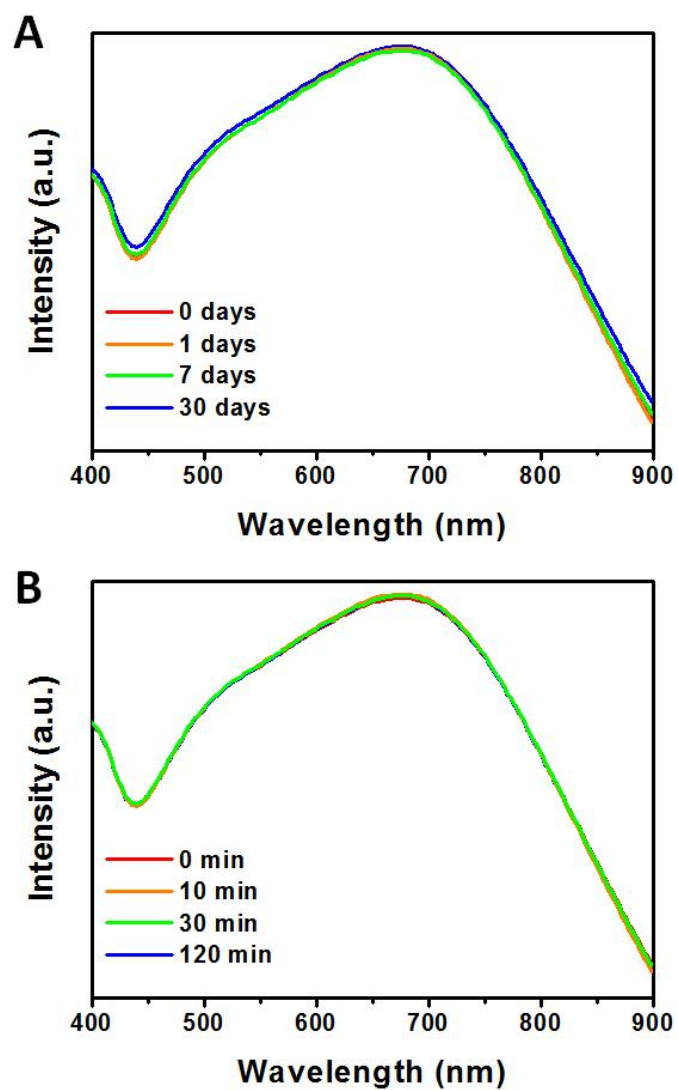


Figure S12. UV-vis-NIR spectra of NaDyF₄:10%Nd-GA-Fe within 30 days standing A) and 120 min irradiation (1.5 W cm^{-1}) under 808 nm laser B) under pH = 7.5 condition.

Table S2. The evolution of particle size and polydispersity index of NaDyF₄:10%Nd-GA-Fe as a function of time.

| Condition | 0 | PDI | 1 day | PDI | 7 days | PDI | 30 days | PDI |
|-------------|-----|-------|--------|-------|--------|-------|---------|-------|
| standing | 8.7 | 0.059 | 8.4 | 0.041 | 8.7 | 0.042 | 8.3 | 0.051 |
| Condition | 0 | PDI | 10 min | PDI | 30 min | PDI | 120 min | PDI |
| irradiation | 8.5 | 0.026 | 8.9 | 0.038 | 8.8 | 0.059 | 9.2 | 0.082 |

Table S3. The evolution of particle size and polydispersity index of NaDyF₄:10%Nd-GA-Fe as a function of time in serum, PBS, and DMEM.

| Condition | 0 | PDI | 1 day | PDI | 7 days | PDI | 30 days | PDI |
|-------------------|-----|-------|-------|-------|--------|-------|---------|-------|
| standing in serum | 8.6 | 0.028 | 8.9 | 0.052 | 8.8 | 0.072 | 9.4 | 0.074 |
| standing in PBS | 8.4 | 0.048 | 8.9 | 0.022 | 8.7 | 0.075 | 9.3 | 0.094 |
| standing in DMEM | 8.0 | 0.046 | 8.6 | 0.047 | 8.9 | 0.053 | 9.0 | 0.085 |

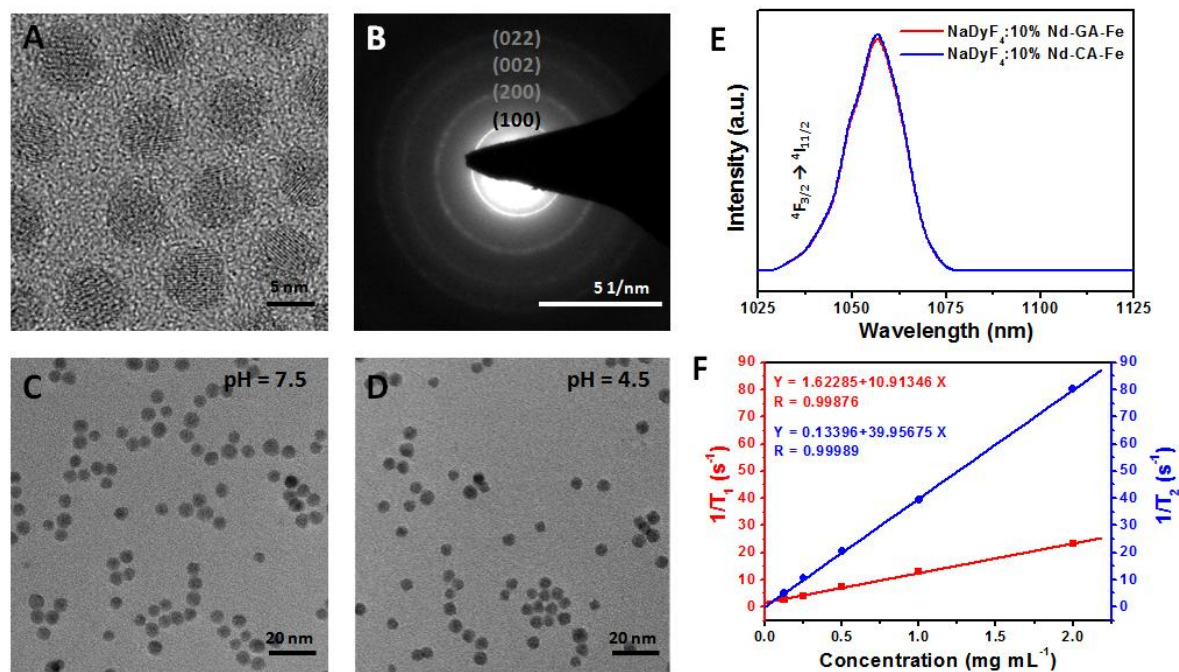


Figure S13. HR-TEM images A) and SAED pattern B) of NaDyF₄:10%Nd-CA. C,D) TEM images of NaDyF₄:10%Nd-CA-Fe in different pH condition (pH = 7.5 and 4.5). E) NIR II DCL spectra of NaDyF₄:10%Nd-CA-Fe and NaDyF₄:10%Nd-GA-Fe. F) Relaxation rate ($1/T_1$ and $1/T_2$) vs various mass concentrations of NaDyF₄:10%Nd-CA-Fe at room temperature using a 0.5 T MRI scanner.

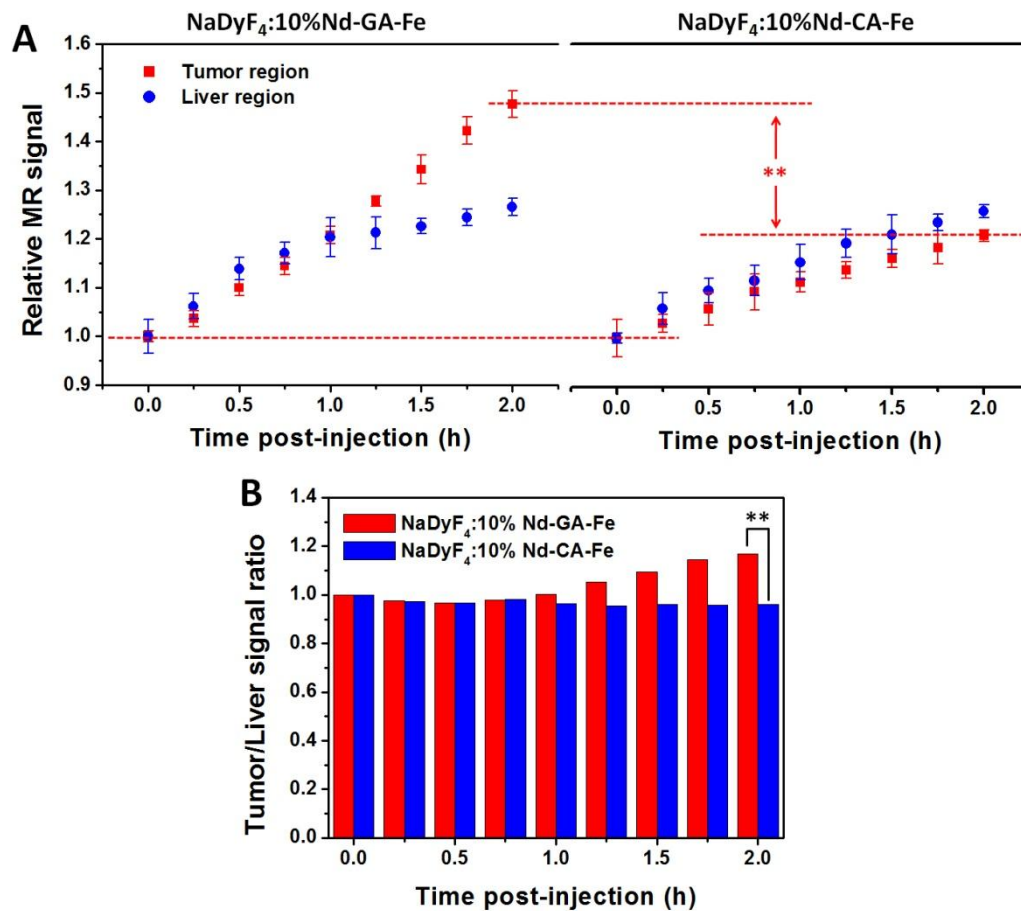


Figure S14. T₂-weighted MRI signals in tumor and liver region A) and Tumor/liver signal ratio of T₂-weighted MRI signal B) after intravenous injection of NaDyF₄:10%Nd-GA-Fe. NaDyF₄:10%Nd-CA-Fe was used for comparison.

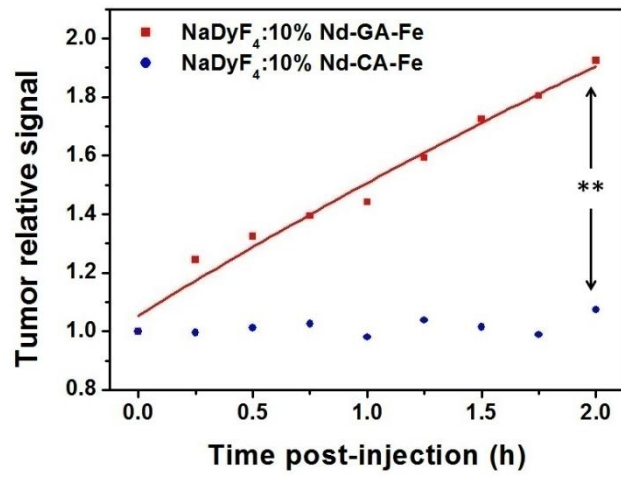


Figure S15. NIR II DCL signal in tumor region after intratumorous injection of NaDyF₄:10%Nd-GA-Fe. NaDyF₄:10%Nd-CA-Fe was used for comparison.

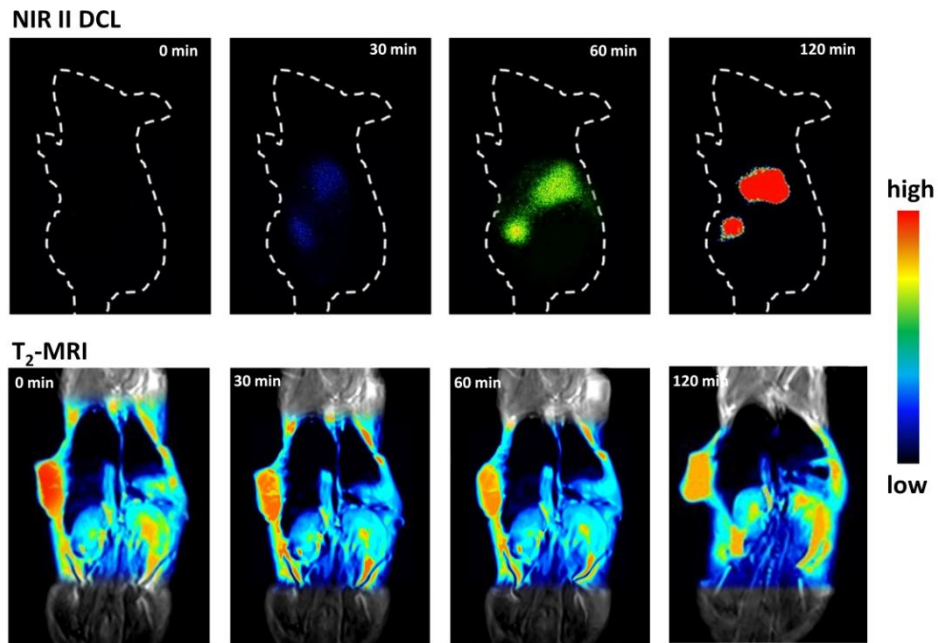


Figure S16. NIR II DCL images (upper) and T₂-weighted MRI images (lower) at different times point post-injection.

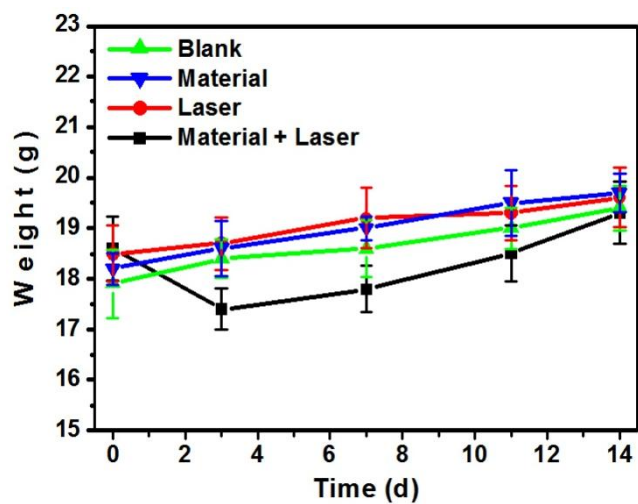


Figure S17. The bodyweight change of mice during the PTT.

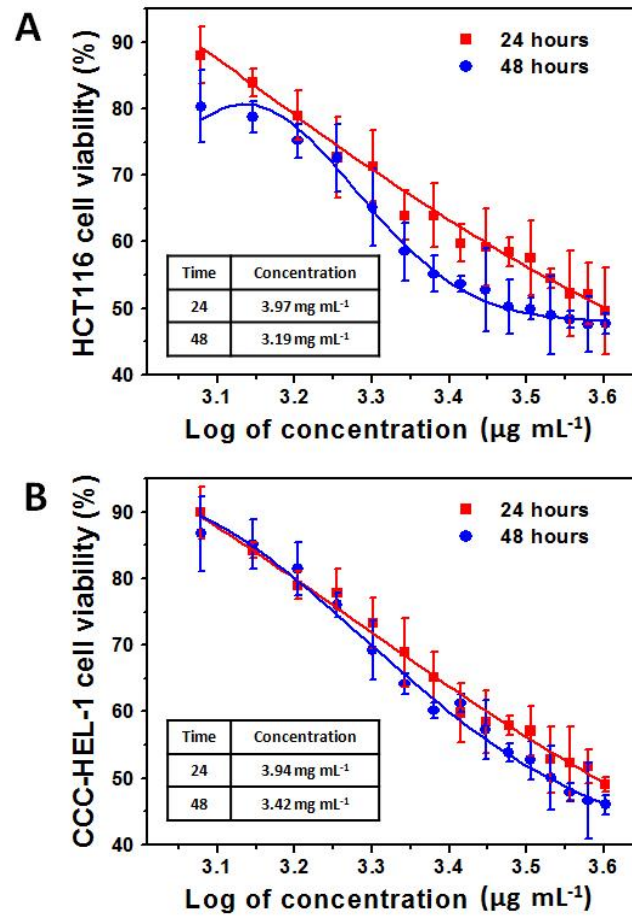


Figure S18. Half maximal (50%) inhibitory concentration (IC₅₀) of NaDyF₄:10%Nd-GA-Fe incubated for 24 and 48 hours.

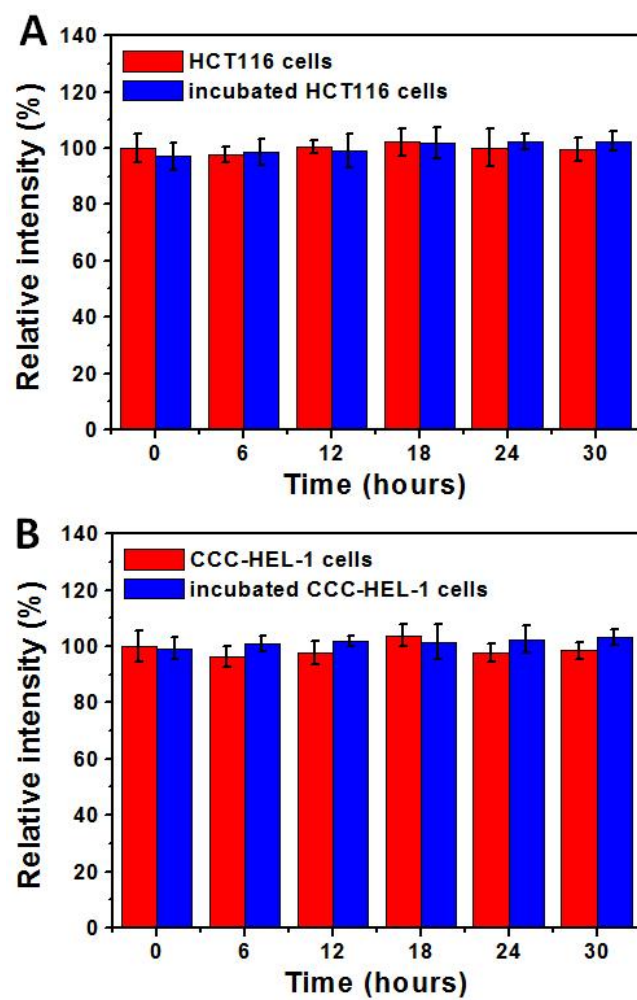


Figure S19. The relative ROS amount of NaDyF₄:10%Nd-GA-Fe incubated HCT116 A) and CCC-HEL-1 B) cells vs time. The ROS amount of untreated cells at 0 hour was defined as 100%.

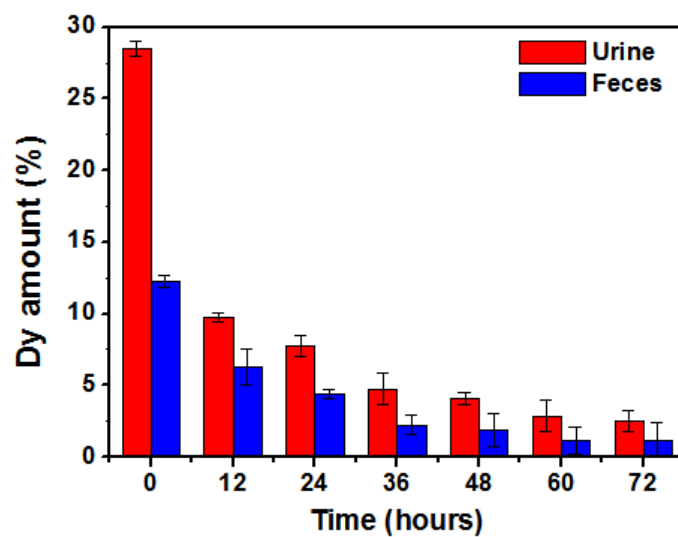


Figure S20. The Dy amount in mice urine and feces at various time point after injection of NaDyF₄:10%Nd-GA-Fe.

Calculation of the molar extinction coefficient.

The extinction coefficient (ϵ) can be determined:

$$\epsilon = \frac{AV_{\text{NPs}}\rho N_{\text{A}}}{LC} \quad (\text{S1-1})$$

where ϵ is the molar extinction coefficient, A is the absorption at a wavelength of 808 nm of nanoparticles, V is the average volume of the nanoparticles, ρ is the density of nanoparticles, N_{A} is Avogadro's constant, L is the path length (1 cm), and C is the weight concentration of the nanoparticles.

Calculation of the photothermal conversion efficiency.

The photothermal conversion efficiency (η) can be determined:

$$\eta = \frac{hA\Delta T_{\max} - Q_s}{I(1 - 10^{-A_\lambda})} \quad (\text{S2-1})$$

where η is the photothermal conversion efficiency from the absorbed light energy to thermal energy, h is the heat transfer coefficient, A is the surface area of the container, ΔT_{\max} is the temperature change at the maximum steady-state temperature, Q_s is the heat associated with the light absorbance of the solvent, which is measured using pure water, I is the laser power, and A_λ is the absorbance of NaDyF₄:10%Nd-GA-Fe at the wavelength of 808 nm.

In the Equation S2-1, only hA is unknown for calculation. In order to get the value of hA , θ is introduced, which is defined as the ratio of ΔT to ΔT_{\max} :

$$\theta = \frac{\Delta T}{\Delta T_{\max}} \quad (\text{S2-2})$$

Where ΔT is the temperature change, which is defined as $T - T_{\text{surr}}$ (T and T_{surr} are the solution temperature and ambient temperature of the surroundings, respectively). Thus, hA can be determined as following:

$$hA = \frac{mC_p}{\tau} \quad (\text{S2-3})$$

Where τ is the slope of the linear time data from the cooling period vs $-\ln\theta$ (Figure S9). m and C_p are the mass and heat capacity of water, respectively.